HHS Public Access

Author manuscript

Clin Cancer Res. Author manuscript; available in PMC 2018 November 02.

Published in final edited form as:

Clin Cancer Res. 2018 January 01; 24(1): 169–180. doi:10.1158/1078-0432.CCR-17-1318.

Hypoxia-inducible PIM kinase expression promotes resistance to anti-angiogenic agents

Andrea L. Casillas[#1], **Rachel K. Toth**[#2], **Alva G. Sainz**[3], **Neha Singh**[3], **Ankit A. Desai**[4], **Andrew S. Kraft**[2,4], and **Noel A. Warfel**[2,5,*]

[1]department of Cancer Biology, University of Arizona

[2]University of Arizona Cancer Center

[3]Biological and Biomedical Sciences graduate program, Yale University

[4]Department of Medicine, University of Arizona

[5]Department of Cellular and Molecular Medicine, University of Arizona

[#] These authors contributed equally to this work.

Abstract

Purpose: Patients develop resistance to anti-angiogenic drugs, secondary to changes in the tumor microenvironment, including hypoxia. PIM kinases are pro-survival kinases and their expression increases in hypoxia. The goal of this study was to determine whether targeting hypoxia-induced PIM kinase expression is effective in combination with VEGF-targeting agents. The rationale for this therapeutic approach is based on the fact that anti-angiogenic drugs can make tumors hypoxic, and thus more sensitive to PIM inhibitors.

Experimental Design: Xenograft and orthotopic models of prostate and colon cancer were used to assess the effect of PIM activation on the efficacy of VEGF-targeting agents. Immunohistochemistry and *in vivo* imaging were used to analyze angiogenesis, apoptosis, proliferation, and metastasis. Biochemical studies were performed to characterize the novel signaling pathway linking PIM and HIF-1.

Results: PIM was upregulated following treatment with anti-VEGF therapies, and PIM1 overexpression reduced the ability of these drugs to disrupt vasculature and block tumor growth. PIM inhibitors reduced HIF-1 activity, opposing the shift to a pro-angiogenic gene signature associated with hypoxia. Combined inhibition of PIM and VEGF produced a synergistic antitumor response characterized by decreased proliferation, reduced tumor vasculature, and decreased metastasis.

Conclusions: This study describes PIM kinase expression as a novel mechanism of resistance to anti-angiogenic agents. Our data provide justification for combining PIM and VEGF inhibitors to treat solid tumors. The unique ability of PIM inhibitors to concomitantly target HIF-1 and

[*]To whom correspondence should be addressed: Noel A. Warfel, 1515 N. Campbell Avenue, Levy Cancer Center, Rm 0985 Tucson, Arizona 85724, Tel: 520-626-7756, Fax: 520-626-4230, warfelna@email.arizona.edu.

Conflict of Interest: The authors disclose no conflicts of interest

selectively kill hypoxic tumor cells addresses two major components of tumor progression and therapeutic resistance.

Keywords

PIM kinases; HIF-1; Angiogenesis; VEGF; anti-angiogenic agents

Introduction

Angiogenesis is a hallmark of tumorigenesis that is required for tumor growth and metastasis (1, 2). The recognition of vascular endothelial growth factor (VEGF) as an important stimulator of angiogenesis and subsequent tumor growth has led to the clinical development of VEGF and VEGF receptor (VEGFR) inhibitors (3). In the past decade, small-molecule receptor tyrosine kinase (RTK) inhibitors (e.g., sunitinib) that block the kinase domain of VEGFR and other kinases and a humanized monoclonal antibody that specifically recognizes and blocks VEGF-A (bevacizumab), have been approved for use in various cancer types (4). Clinical trials combining bevacizumab with chemotherapy demonstrated clinical efficacy, prolonging progression-free and overall survival. This combination is currently approved for use in colorectal, lung, and renal cancers, among others (5–7). In the clinical setting, three vascular responses to anti-angiogenic drugs have been described: reduced perfusion (inducing hypoxia), no change, and increased perfusion (vascular normalization). Among these, reduced perfusion is an early and the most frequently identified response (8–10). Consistent with reduced perfusion and increasing hypoxia, many studies reported increased expression of hypoxia-inducible factor (HIF)-1 and carbonic anhydrase 9 (CAIX), as well as a hypoxic gene signature following treatment with anti-angiogenic agents (11, 12). The growth inhibitory effect of anti-angiogenic agents in solid tumors is typically short lived due to *de novo* and acquired resistance (13).

HIF-1 is considered a master regulator of the cellular response to hypoxia, and its activation is largely dependent on the protein level of HIF-1α and HIF-2α, whose expression is regulated in an oxygen-dependent manner. In the presence of oxygen, HIF-1α is hydroxylated on prolines 402 (Pro402) and 564 (Pro564) by prolyl hydroxylase domain-containing proteins (PHDs) (14, 15). Following hydroxylation, HIF-1α is recognized by von Hippel-Lindau (VHL), an E3 ubiquitin ligase, which leads to its ubiquitination and degradation by the 26S proteasome (16, 17). Under hypoxic conditions, HIF-1/2α are not degraded efficiently, allowing the protein to accumulate and enter the nucleus. The activation of HIF-1 induces the transcription of multiple genes that promote cellular processes that are necessary for tumorigenesis, including angiogenesis (18, 19). Prolonged activation of HIF-1 is associated with resistance to anti-angiogenic agents (20). Thus, identifying signaling molecules that control HIF-1 expression is critical for our understanding of therapeutic resistance and developing effective strategies to target tumor angiogenesis.

The Proviral Integration site for Moloney murine leukemia virus (PIM) kinases are a family of oncogenic Ser/Thr kinases that are frequently overexpressed in various types of cancer (21, 22). PIM1 expression is elevated in ~50% of human prostate cancer specimens, particularly in advanced disease (22, 23). PIM1 promotes tumor progression by impacting

cell cycle progression, proliferation, and survival (24). As a result, PIM has been the focus of drug development efforts, and several small molecule pan-PIM inhibitors are currently being tested in clinical trials (25, 26). Our group recently described that PIM protein levels increase in response to hypoxia, and PIM inhibitors selectively kill hypoxic cancer cells, indicative of the importance of PIM expression for the adaptation of tumor cells to hypoxia (27). Here, we investigate the consequence of altered PIM1 expression on the tumor microenvironment and efficacy of anti-angiogenic agents.

Materials and Methods

Plasmids and siRNA

HA-HIF-1α (28), HRE-Luc (29), ODD-Luc (30), CMV-Luc, and SV40-Luc (31) constructs were purchased from Addgene. The ODD-Luc (P564A) mutant was created using a Quikchange site directed mutagenesis kit (Agilent). Renilla-Luc (pRL4-Luc) was purchased from Promega. EGFP-HIF-1 α and HA-Ubiquitin were gifts from Dr. Wafik El Deiry (Fox Chase Cancer Center) and Dr. Alexandra Newton (UCSD), respectively.

Reagents and antibodies

The anti-murine anti-VEGF monoclonal antibody B20–4.1.1 (B20) was provided by Genentech. AZD1208 and LGB-321 were acquired from AdooQ Biosciences, and sunitinib malate was obtained from Selleck Chemicals. Cycloheximide, MG-132, dimethyloxalylglycine (DMOG), and doxycycline were purchased from Sigma. Calcein AM was purchased from Invitrogen. The antibody against HIF-2α was purchased from Novus. Antibodies to HIF-1α, VHL, and VEGF were purchased from BD Transduction Laboratories. PIM1/2/3, phospho-IRS1 (S1101), HIFOH (P564), cleaved caspase 3 (CC3), and actin antibodies were purchased from Cell Signaling Technology. PIM1, CD31, and Ki67 antibodies used for immunohistochemistry were purchased from Abcam. An anti-HA monoclonal antibody was purchased from Covance, and the anti-pimonidazole mAb (Hypoxyprobe-1) was purchased from Hypoxyprobe, Inc. The GFP antibody was purchased from Sigma. All other materials and chemicals were reagent-grade.

Cell transfection and immunoblotting

PC3, HCT116, and PC3-LN4 cell lines were maintained in RPMI medium (Cellgro) containing 10% FBS (Hyclone). 293T cells, wild types (WT) mouse embryonic fibroblasts (MEFs), tripleknockout (TKO; $Pim1^{-/-}$, $Pim2^{-/-}$, and $Pim3^{-/-}$ (32)) MEFs, TKO MEFs stably expressing PIM1, PIM2, or PIM3 (33), and 786–0 renal cancer cells stably expressing PRC3 (vector) or WT8 (Wild-type VHL) (34) were maintained in DMEM containing 10% FBS and 1% penicillin/streptomycin. Human umbilical vein endothelial cells (HUVECs) were cultured in complete EBM-2 media containing 10% FBS (Lonza). All cell lines were maintained at 37°C in 5% CO_2 and were authenticated by short tandem repeat DNA profiling performed by the University of Arizona Genetics Core Facility. The cell lines were used for less than 50 passages, and were routinely tested for mycoplasma contamination. When indicated, cells were maintained in a hypoxic environment (1.0% O_2) using a hypoxia workstation (In vivo2 400, Ruskinn, Bridgend, UK). Transient transfection was carried out using Lipofectamine 3000 (Thermo Fisher), according to the manufacturer's protocol.

Immunoblotting and ubiquitination assays were performed as described previously (35). Densitometric analysis was performed with ImageJ analysis software.

qRT-PCR analysis

Hypoxia-responsive gene expression was measured using RT^2 hypoxia-signaling PCR profiler arrays (Qiagen). All other qRT-PCR reactions were performed using Biorad SsoAdvanced Universal SYBR green supermix, according to the manufacturer's protocol. Validated primer sets (QuantiTech primer assays; Qiagen) for each of the following genes were purchased to measure gene expression: VEGF-A, glucose transporter type-1 (SLC2A1), angiopoietin like 4 (ANGPTL4), and hexokinase 2 (HK2).

Tube formation assays

Tissue culture media was collected under the specified conditions and centrifuged to pellet cellular debris. Early passage (< p8) HUVECs were suspended in conditioned media, plated on Matrigel-coated wells, and tube formation was imaged over time. Fifteen minutes prior to imaging, Calcein AM (2 μM) was added to each well. Tube length and total branches were quantified using WimTube angiogenesis image analysis software (Wimasis).

Subcutaneous and orthotopic implantation

For xenograft studies, PC3-LN4, HCT116, SW620, or PC3 cell lines were injected subcutaneously into the rear flank of mice in PBS/Matrigel (v/v). Once tumors reached a volume of approximately 150 mm3, the mice were randomized for treatment with vehicle, AZD1208 (30 mg/kg/day by p.o. daily), sunitinib (80 mg/kg by p.o. daily), B20 (5 mg/kg by i.p every other day), or the indicated combinations. Tumor volumes were monitored over time by caliper measurement. For *in vivo* vascular imaging, mice were injected with 2 nmol Angiosense 750EX (PerkinElmer) and imaged at 24 h. For the orthotopic prostate model, 5×10^5 PC3-LN4 cells were injected into the ventral lobe of the prostate. For the orthotopic colon model, 5×10^5 HCT116 cells were injected into the cecum (36). At the conclusion of all *in vivo* experiments, mice were injected with pimonidazole (60 mg/kg by i.p.) 45 minutes prior to sacrifice to mark hypoxic tissue. After harvest, tumors were fixed, embedded in paraffin, and sectioned for staining with hematoxylin and eosin (H&E) or antibodies specific for PIM1, CD31, Ki67, cleaved Caspase-3 (CC3), and Hypoxyprobe-1 (HP-1). Independent investigators blinded to the identity of the samples scored CD31 and CC3 by manual counting. Percent HP-1, Ki67, and PIM1 positive staining was calculated using Image J analysis software. All animal studies were approved by the Institutional Animal Care and Use Committee at the University of Arizona.

Statistical analysis

All western blots are representative of at least three independent experiments. Differences between groups were determined by Student's t-test and linear regression analysis. Two-way ANOVA was used to analyze differences between groups with two independent variables. *P* values were adjusted using Tukey adjustment. For *in vivo* experiments, univariate crosssectional analyses compared tumor volume by treatment group using the Wilcoxon Rank Sum Rank Test. After cube root transformations to achieve approximate normality,

multivariate analysis compared tumor volume by day of observation, measurement time, and treatment using mixed effects models that accounted for the correlations between the measurements obtained over time for individual mice. All analyses used STATA 15. All data are presented as the mean ± SE, and a $P < 0.05$ was considered to be statistically significant.

Results

PIM1 expression is increased in response to anti-angiogenic agents.

Anti-angiogenic drugs are designed to disrupt the tumor vasculature, which often leads to hypoxia. We recently reported that the protein levels of PIM kinases increase following exposure to hypoxia (27). Therefore, we hypothesized that PIM expression might increase in tumor cells following treatment with anti-angiogenic agents. To test this theory, 1×10^6 PC3 cells were implanted into the flanks of male NSG mice. Once tumors were established, the mice were treated with vehicle, sunitinib, or the murine anti-VEGF antibody, B20. Prior to sacrifice, the mice were injected with pimonidazole as a marker for hypoxia. Treatment with B20 or sunitinib significantly increased HP-1 staining compared to vehicle-treated tumors, indicative of extensive hypoxia (Fig 1A and B). Moreover, expression of CAIX, a hypoxia-inducible gene, significantly increased following treatment, indicating that anti-VEGF agents increase hypoxia in these tumors (Fig S1). Consistent with previous reports, PIM1 protein exhibited a nuclear staining pattern with variable cytoplasmic staining (37, 38). Treatment with B20 or sunitinib significantly increased PIM1 levels compared to vehicle treatment, reaching over 60% positive staining following B20 treatment (Fig. 1C). Notably, PIM1 levels visibly overlapped with regions of hypoxia in serial sections, regardless of treatment group (Fig 1A). Next, tumor tissues were lysed, and immunoblotting was used to assess the protein levels of each PIM isoform following treatment. PIM1 and PIM2 levels were consistently higher in tumors treated with either B20 or sunitinib, whereas PIM3 levels remained relatively constant (Fig 1D).

Because PIM is upregulated in response to anti-VEGF therapies and known to enhance cancer cell survival in hypoxia (27), we tested whether PIM1 overexpression, which is a frequent event in many cancers, is sufficient to impart *de novo* resistance to anti-angiogenic drugs. To test this theory, we generated prostate cancer cell lines stably expressing PIM1 and performed xenograft experiments to assess the ability of sunitinib and B20 to inhibit tumor growth and vasculature. One million PC3/VEC or PC3/PIM1 cells were implanted subcutaneously into the flanks of male NSG mice. Once tumors were established, the mice were treated with vehicle, sunitinib, or B20, and tumor volume was measured over time. Verifying previous reports, PIM1 overexpressing tumors grew significantly larger than control tumors (39) (Fig 1E). In PC3/VEC tumors, sunitinib and B20 significantly reduced tumor growth by 38% and 46%, respectively. In contrast, neither drug significantly reduced the volume of PC3/PIM1 tumors (Fig. 1F). Thus, PIM1 expression significantly reduced the growth-inhibitory effect of anti-angiogenic agents *in vivo*. To assess whether PIM1 impacts the vascular response of tumors to sunitinib and B20, tumor tissues were stained with CD31 to measure angiogenesis. B20 and sunitinib significantly reduced microvessel density (MVD) in PC3/VEC tumors, whereas neither agent significantly decreased MVD in the PC3/PIM1 tumors (Fig. S2). This result suggests that PIM1-expressing tumors are able to

maintain functional vasculature during treatment with anti-VEGF therapies. Taken together, these data indicate that PIM levels are increased following treatment with B20 or sunitinib, and PIM1 expression impairs the ability of anti-angiogenic agents to inhibit tumor vasculature formation and tumor growth.

Combining PIM and VEGF inhibitors yields synergistic anti-tumor activity.

Based on our previous discovery that PIM is critical for tumor cell survival in hypoxia, we reasoned that inhibiting PIM in combination with anti-angiogenic agents could be an effective strategy for therapy. The rationale for this therapeutic approach is based on the fact that anti-angiogenic drugs starve the tumor of oxygen, making it more hypoxic and thus more sensitive to PIM inhibitors. PC3-LN4 cells were injected subcutaneously into each flank of male NOD-SCID mice, and tumors were allowed to grow to an average size of 150 mm^3. Then, the mice were randomly segregated into the indicated treatment groups. AZD1208 (AZD, a pan-PIM kinase inhibitor), was used at the maximum tolerated dose, and dose response experiments were performed with B20 to identify a suitable dose for combination treatment (Fig. S3). Treatment with AZD or B20 alone showed moderate inhibition of tumor growth, ranging from 32% to 48% at the experiments end. Strikingly, combining AZD and B20 significantly blocked tumor growth by 94% (Fig. 2A). Similar results were observed using sunitnib (RTK/VEGFR inhibitor), indicating that the effect was not drug-specific (Fig. S4A). Next we tested the efficacy of AZD+B20 in models of colon cancer, where Bevacizumab is actively used in patients. Combined inhibition of VEGF and PIM significantly reduced tumor volume in xenograft models using HCT116 and SW620 colon cancer cell lines (Fig. S4B and C). To investigate whether the response to AZD+B20 was stable, SW620 xenografts were treated for 13 days and then treatment was stopped. Tumor regrowth was measured for each cohort until tumors reached an average volume of 1000 mm^3. Combined inhibiton of PIM and VEGF not only reduced tumor volume during treatment, but AZD+B20-treated tumors grew at a signficantly slower rate after drug withdrawal compared to naïve, vehicle-treated tumors (Fig. S4C). To measure tumor vasculature in each cohort, mice were injected with Angiosense750EX, a fluorescent probe that remains localized in the vasculature to allow for *in vivo* imaging of angiogenesis. To calculate the relative amount of functional vasculature in each cohort, Angiosense signal was normalized to differences in tumor volume to obtain a vascular index for each treatment group. Treatment with AZD+B20 decreased vascular perfusion to a greater extent than B20 alone, suggesting that PIM activity can help preserve tumor vasculature in response to VEGF inhibition (Fig. 2B). CD31 staining confirmed our imaging results; simultaneous inhibition of PIM and VEGF significantly reduced MVD compared to either agent alone (Fig 2C and2D). To measure cell death and proliferation, tumor sections were stained with CC3 and Ki67, respectivley. AZD or B20 alone produced no significant increase in cell death and only a modest reduction in proliferation. In contrast, CC3 staining was 3-fold higher in tumors from mice treated with the combination compared with B20 alone (Fig 2D), and there was a dramatic reduction in Ki67-positive cells in the AZD+B20 tumors (Fig. 2E). Thus, the anti-tumor effect of combined inhibiton of VEGF and PIM is characterized by a significant reduction in angiogenesis and proliferation, as well as increased cell death.

Inhibition of PIM alters the transcriptional response to hypoxia and reduces angiogenesis

Hypoxia is known to activate a pro-angiogenic gene expression signature in human tumors that promotes neovascularization (40). To investigate the influence of PIM activity on the cellular response to hypoxia, we assessed the effect of PIM inhibition on a panel of 84 hypoxiainducible genes. PC3-LN4 prostate cancer cells were cultured in normoxia or hypoxia ± AZD1208 for 8 h, and mRNA was collected for subsequent gene expression analysis. Exposure to 1.0% O_2 altered the transcript levels of several classes of hypoxia-responsive genes, including critical mediators of angiogenesis (Fig 3A). To identify genes that could be controlled by PIM, we focused on genes that were upregulated by at least 2.5-fold in hypoxia and were significantly reduced by treatment with AZD. Thirteen genes that fit these criteria, 7 of which are known to promote angiogenesis, and all are established targets of the HIF-1 transcription factor (Fig. 3B). The inhibitory effect of AZD on several hypoxia-inducible genes involved in angiogenesis (ANGPTL4 and VEGFA) and metabolism (SLC2A1 and HK2) was validated by qRT-PCR (Fig. S5). Thus, PIM inhibition impairs the ability of cancer cells to induce a proangiogenic gene signature in response to hypoxia.

Next, *in vitro* angiogenesis assays were performed to determine whether PIM inhibition could limit the release of hypoxia-induced pro-angiogenic factors from cancer cells. PC3 prostate cancer cells were cultured in normoxia or hypoxia for 24 h in the presence or absence of AZD, and cell lysates and conditioned media (CM) were collected. Immunoblotting of cell lysates verified that PIM1, PIM2, HIF-1α and HIF-2α protein levels increased in response to hypoxia. Strikingly, treatment with AZD decreased the expression of HIF-1α and HIF-2α (Fig. 3C). To assess the importance of PIM for hypoxia-induced angiogenesis, HUVECs were suspended in conditioned media (CM) from each experimental condition, plated on Matrigel, and tube formation was assessed over time. Fluorescence images of Calcein AM-stained endothelial cells were acquired at 0, 3, and 6 h, the last of which corresponded with maximal tube formation. Compared to CM from untreated cells, CM from cells treated with AZD in normoxia did not significantly affect tube formation, indicating that the PIM inhibitor does not acutely affect HUVEC viability or their ability to form tubes (Fig 3D, left panels). As expected, CM from hypoxic cells substantially enhanced tube formation compared to CM from normoxic cells (Fig 3D, top panels). Strikingly, the pro-angiogenic effect of hypoxia was abolished in CM from cells in hypoxia treated with AZD (Fig. 3D, right panels). Image analysis verified that hypoxia significantly increased average tube length and the number of branch points, and inhibition of PIM largely blocked the hypoxia-mediated increase in tube formation (Fig. 3E and 3F). Taken together, these data indicate that PIM inhibitors blunt HIF-1 activation and reduce hypoxia-induced angiogenesis.

PIM inhibitors reduce HIF- 1/2a protein stability by increasing its proteasomal degradation.

Activation of the HIF-1 transcription factor is directly correlated with the protein levels of HIF-1/2α (15, 41). Thus, we tested whether the reduction in HIF-1/2α protein observed with AZD treatment was sufficient to reduce HIF-1 activity in cancer cells. PC3-LN4 cells were cotransfected with Renilla-Luc and HRE-Luc, and incubated in hypoxia for 6 h with two chemically distinct pan-PIM inhibitors (AZD1208 or LGB-321). To account for cell death or growth inhibition in response to PIM inhibitor treatment, the HRE-Luc signal was

normalized to Renilla-Luc levels. Both inhibitors significantly reduced HIF-1 activity in a dose-dependent manner (Fig. 4A). To confirm that the effects of these small molecules on HIF-1 were due to the loss of PIM activity, WT or TKO MEFs (32) stably expressing PIM1, PIM2, or PIM3 were placed in hypoxia for 6 h, and protein was collected to analyze HIF-1/2α levels. TKO MEFs displayed lower levels of HIF-1α and HIF-2α protein compared to WT MEFs, and restoring the expression of any of the PIM isoforms was sufficient to rescue HIF-1/2α to the levels observed in WT MEFs; overexpression of PIM1 and PIM2 caused further accumulation (Fig 4B). Moreover, the hypoxia-induced expression of HIF-1 target genes, *GLUT1* and *VEGF*, was significantly blunted in TKO MEFs (Fig. S6). These data demonstrate that genetic or chemical inhibition of PIM significantly lowers HIF-1/2α protein levels and reduces HIF-1 activity in hypoxia.

To investigate the mechanism by which PIM regulates HIF-1, we tested whether PIM activity affects the stability of HIF-1/2α proteins. PC3-LN4 cells were placed in hypoxia for 4 h to allow HIF-1/2α to accumulate, and then cells were then pretreated with DMSO or AZD for 30 min prior to the addition of cycloheximide, a global inhibitor of protein translation. Lysates were collected over a 4 h time course, and HIF-1/2α levels were monitored to determine changes in protein half-life (Fig. 4C). HIF-1α and HIF-2α were turned over at a significantly faster rate in the presence of AZD compared to DMSO ($t_{1/2}$ HIF-1α = 0.5 ± 0.1 h vs. 2.2 ± 0.2; $t_{1/2}$ HIF-2α = 1.7 ± 0.2 h vs. 6.2 ± 0.4), suggesting that loss of PIM activity increases the rate of degradation (Fig. 4C). Next, we tested whether PIM inhibitors promote the degradation of HIF-1/2α through the proteasome. PC3-LN4 prostate cancer cells were treated with AZD alone or in combination with MG-132, a proteasome inhibitor, for 6 h under hypoxic conditions. AZD alone significantly decreased HIF-1/2α levels, whereas MG-132 completely abolished the ability of AZD1208 to reduce HIF-1/2α levels, indicating that PIM inhibition reduces HIF-1/2α isoform stability in a proteasome-dependent manner (Fig. 4D). We next explored whether PIM inhibition was accompanied by increased ubiquitination of HIF-1α. 293T cells were co-transfected with GFPHIF-1α and HA-ubiquitin. The next day, cells were placed in hypoxia for 4 h, pretreated with vehicle or AZD for 30 min, followed by treatment with MG-132 for 0, 1, or 3 hours. HIF-1α was immunoprecipitated using an anti-GFP antibody, and the amount of ubiquitin linked to HIF-1α was detected by immunoblotting. The amount of HA-ubiquitin bound to HIF-1 α increased in cells treated with AZD compared to DMSO (Fig 4E). Quantitation of the signal in the region above HIF-1α (indicated by a bracket), normalized to total HIF-1α, revealed a 3-fold increase in ubiquitination after 3 h treatment with AZD compared to vehicle, demonstrating that PIM inhibition increases HIF-1α ubiquitination (Fig. 4F). Confirming successful inhibition of PIM, phosphorylation of a PIM substrate, IRS1 (S1101), was completely blocked by AZD1208 treatment (Fig. 4F). Taken together, these data demonstrate that PIM inhibition promotes the ubiquitination and degradation of HIF-1/2α by the 26S proteasome in hypoxia.

PIM kinase activity blocks the hydroxylation of HIF-1/2α by PHDs.

HIF-1/2α proteins are turned over through a well-defined pathway that involves hydroxylation by PHDs, binding to VHL, and subsequent degradation by the 26S proteasome (42). To decipher the mechanism of PIM inhibitor action, we evaluated the

functionality of each player involved in this HIF degradation pathway. First, we examined the role of VHL using 786-O renal carcinoma cells, which lack VHL and constitutively express HIF-2α, stably expressing vector (PRC3) or wild-type VHL (WT8) (34). These cell lines were placed in normoxia or hypoxia for 6 h ± AZD, and western blotting was used to monitor HIF-2α protein levels. As expected, HIF-2α was expressed in normoxic conditions in PRC3 cells, but not in WT8 cells expressing VHL. HIF-2α was refractory to AZD treatment in PRC3 cells but was significantly reduced by AZD in WT8 cells, indicating that VHL is necessary for AZD to reduce HIF-2α (Fig. 5A). Next, we asked whether PHDs were required for AZD to reduced HIF-1/2α levels. PC3-LN4 cells were treated with AZD alone or in combination with DMOG (a PHD inhibitor), for 6 h in hypoxia. AZD alone decreased HIF-1/2α levels, whereas simultaneous treatment with DMOG restored HIF-1/2α protein to basal levels, indicating that PIM inhibition requires PHD activity to reduce HIF-1/2α (Fig. 5B). This conclusion is supported by previously published results showing that a mutant of HIF-1α that cannot be hydroxylated (P402/564A) is refractory to AZD1208-mediated downregulation (27). To confirm that PIM influences the ability of PHDs to act on HIF-1α, the extent of HIF-1α hydroxylation was evaluated in WT and TKO MEFs after treatment with MG-132 (prevents hydroxylated HIF-1α from being degraded) or DMOG. While TKO MEFs accumulated slightly less total HIF-1α during MG-132 treatment, they had significantly more hydroxylated HIF-1α (Fig. 5C; compare lanes 2 and 5), suggesting that hydroxylation of HIF-1α is enhanced in cells lacking PIM. Next, PHD activity was measured using a previously described PHD activity reporter (ODD-Luc) (30). PC3-LN4 cells were transfected with ODD-Luc or an ODD-Luc (P564A) mutant that is not responsive to oxygen concentration (P564A-Luc). The cells were incubated in normoxia or hypoxia for 6 h ± AZD or LGB-321, and luciferase expression was calculated relative to normoxia. Luminescence was unchanged in cells expressing ODDLuc (P564A), regardless of hypoxia or drug treatment. However, in cells expressing ODD-Luc, luminescence increased by over 3-fold in hypoxia, and both PIM inhibitors reduced the signal to normoxic levels (Fig. 5D), indicating that the ability of PHDs to hydroxylate HIF-1α is increased when PIM is inactive. To confirm that PIM influences HIF-1α at the level of hydroxylation, we compared the effects of hypoxia and DMOG on the accumulation of HIF-1/2α in WT and TKO MEFs. We predicted that if PIM were acting at the level of PHDs, DMOG treatment would negate the difference in HIF-1/2α protein levels observed in WT and TKO MEFs. Both cell lines were subjected to hypoxia or DMOG treatment, and protein was collected at the indicated time points to compare HIF levels. HIF-1/2α accumulated more quickly in WT compared to TKO MEFs in hypoxia, whereas there was no difference following DMOG treatment at every time point examined (Fig 5E). These results support a model whereby the presence of active PIM reduces the hydroxylation and subsequent degradation of HIF-1/2α.

Combined inhibition of VEGF and PIM reduce metastasis in prostate and colon cancer.

Access to vasculature is required for cancer cells to escape the primary tumor and form metastases. Interestingly, treatment with bevacizumab has been associated with an increase in local invasion and metastasis; despite the fact this drug reduces vasculature (43, 44). Thus, we tested whether combined inhibition of PIM and VEGF could prevent metastasis in orthotopic models of prostate and colon cancer. Male NSG mice were injected in the dorsal lobe of the prostate with 5×10^5 PC3-LN4 cells stably expressing SV40-Luc so that primary

tumor growth could be monitored over time using BLI. Seven days post-injection, tumor growth was verified by luminescence, and all mice with primary tumors were randomly segregated into four treatment groups: vehicle, AZD, B20, and AZD+B20. Mice were imaged weekly thereafter, and luminescence was used as a measure of tumor volume. Treatment with B20 or AZD alone did not alter tumor growth, whereas AZD+B20 reduced tumor volume by approximately 40% by the end of the study (Fig 6A). Confirming the results of our bioluminescence imaging, there was no significant reduction in tumor weight in mice treated with B20 or AZD compared to the control group, whereas prostates from mice treated AZD+B20 were visibly smaller and weighed significantly less than all other cohorts (Fig 6B and C). At the end of the study, necropsy was performed to quantify metastasis. Macroscopic metastases were present in the lymph nodes and livers of mice from all groups, but treatment with AZD+B20 significantly reduced the incidence of metastases to both organs compared to vehicle (Fig 6D). Interestingly, AZD alone significantly reduced the number of metastases per liver, even though there was no significant reduction in tumor volume in this cohort (Fig. 6E). Impressively, only one liver metastasis was observed among AZD+B20 treated mice, demonstrating that this treatment strategy significantly reduced prostate cancer metastasis (Fig 6E). To validate the anti-metastatic effect of combined PIM and VEGF inhibition, a parallel experiment was performed in an orthotopic model of colon cancer using HCT116 cells. Treatment with AZD+B20 significantly reduced ceca weight and the number of liver metastases compared to vehicle or single agent treatment (Fig. S7). Immunohistochemical staining for HP-1 and PIM1 revealed significant hypoxia in liver metastases from the prostate tumor (Fig. S8). As predicted, PIM1 staining correlated with hypoxic regions toward the center of the tumor (Fig. 6F). These experiments demonstrate that simultaneous inhibition of VEGF and PIM slows primary tumor growth and decreases metastasis in animal models of both colon and prostate cancer (Fig. 6G).

Discussion

The “angiogenic switch” during tumor progression is increasingly recognized as a rate-limiting step in tumorigenesis (45). Most angiogenesis inhibitors used in the treatment of cancer block the action of VEGF. Following a period of clinical benefit, these drugs typically only delay time to progression, which is suggestive of the emergence of resistance. Building on our previous results showing that PIM is critical for survival in hypoxia, we hypothesized that PIM expression might promote resistance to anti-angiogenic agents. The goal of this study was to investigate the role of PIM kinases in mediating tumor angiogenesis and determine whether resistance could be prevented or reversed by inhibition of PIM.

The vascular response of individual tumors to anti-angiogenic therapy can vary over time and between patients. A recent study that aimed to identify intrinsic mechanisms of resistance to bevacizumab in patients with advanced breast cancer using functional imaging reported that nonresponders displayed a higher degree of angiogenesis with more severe hypoxia compared to responders during bevacizumab treatment (46). Based on our results, we anticipate that patients with tumors that contain more severe hypoxia will have elevated PIM which in turn promotes both survival and angiogenesis (Fig 6G). Thus, inhibiting PIM in combination with anti-angiogenic agents negates an intrinsic mechanism of defense within tumor cells. Here, show that combined inhibition of VEGF and PIM kinase elicited a

primarily cytostatic response, as tumors did regrow after drug withdrawal, albeit at a slower rate than naïve tumors (Fig. S4C). Therefore, this regimen would likely need to be combined with a cytotyoxic agent to achieve more durable responses. Results presented suggest that administering PIM inhibitors concomitantly with VEGF inhibitors will target hypoxic tumor cells induced by VEGF inhibition and thus prevent neovascularization. With advances in functional imaging modalities, such as diffusion contrast-enhanced magnetic resonance imaging, acute changes in vascularization can be observed in as little as 5 h after administering bevacizumab (47). Measuring the effect of combined PIM and VEGF inhibition on vascular response might provide a useful strategy to help guide therapy.

Preclinical and clinical studies indicate that tumors often recur with increased invasion or metastasis after anti-angiogenic therapy. However, the mechanisms responsible for this exaggerated aggressiveness are not fully understood. Recent studies have proposed a mechanism of tumor aggressiveness after VEGF inhibition that involves hypoxia, HIF-1α, and the upregulation of RTKs. For example, combined blockade of c-Met and VEGF signaling together reduced tumor invasion and metastasis and prolonged overall survival in mice. Interestingly, this effect was shown to be independent of hepatocyte growth factor, the ligand for c-MET, suggesting that activation occurs through heterodimerization with other RTKs (48). PIM1 was recently described to increase the expression of RTKs in cancer, including c-MET, via the upregulation of protein translation (49). Therefore, targeting PIM could also reduce the compensatory upregulation of c-MET and other RTKs, many of which are transcriptional targets of HIF-1. In an orthotopic model of prostate cancer used in these studies, the incidence of liver metastases was reduced in mice treated with a PIM inhibitor, AZD1208, but not in the cohort treated with the anti-VEGF agent (Fig 6E), even though B20 was more effective at reducing vasculature compared to AZD (Fig 2B). This finding raises the possibility that in addition to their pro-angiogenic effect, PIM kinases might also play a role in regulating hypoxia-induced metastasis. PIM1 was highly expressed in all of the liver metastases examined (Fig 6G), further suggesting that this kinase is active in metastatic cells and represents a viable target for the treatment of patients with advanced cancer who are often diagnosed with metastatic disease.

In response to hypoxia, cancer cells alter gene expression to favor neovascularization. This study is the first to establish a signaling pathway wherein PIM kinases regulate the amplitude of HIF-1 signaling and tumor angiogenesis. Genetic or chemical inhibition of PIM kinase activity reduced the accumulation of HIF-1/2α protein and transcriptional activation of HIF-1. Combined with the fact that PIM kinases are upregulated in hypoxia, this finding poises PIM as a key player in regulating the cellular response to low oxygen. Inhibition of PIM in hypoxia enhanced the hydroxylation of HIF-1 α, initiating its proteasomal degradation (Fig. 4 and 5). Our data fit a model wherein cancer cells increase PIM expression in response to hypoxia to prevent HIF-1/2α degradation, allowing for more rapid and robust activation of HIF-1. Moreover, PIM inhibition decreases HIF-1/2α levels through the canonical PHD-VHL-26S proteasome degradation pathway, even in the context of hypoxia where PHD activity is diminished. Hydroxylation-dependent degradation has been shown to acutely control HIF-1 α levels in hypoxic conditions. For example, it was reported that loss of sirtuin 3 stabilizes HIF-1α in hypoxia by inhibiting PHD activity (50). In addition, several studies demonstrate that decreased mitochondrial oxygen consumption

can elevate intracellular oxygen levels in hypoxia, which is sufficient to enhance PHD function and effectively degrade HIF-α isoforms in hypoxia (51, 52).

In summary, we have described a novel-signaling pathway whereby PIM kinases regulate HIF-1 activation in hypoxia, implicating PIM activation as part of a signaling axis that promotes resistance to anti-VEGF targeted therapies. This study adds additional perspective to our previous data describing the role of PIM in maintaining cell survival in hypoxia via the activation of nuclear factor erythroid 2-related factor 2 (Nrf2) (27). We propose that PIM functions as a hub to control the transcriptional response to hypoxic stress by coordinating signaling through Nrf2 and HIF-1. As a result, inhibiting PIM in solid tumors has the unique advantage of opposing hypoxia by preferentially killing hypoxic tumor cells, while also preventing HIF-1 activation and angiogenesis. Furthermore, we provide preclinical evidence for the use of PIM and VEGF inhibitors in combination to treat solid tumors. Concurrent inhibition of PIM and VEGF maintained the advantageous growth inhibitory effects of angiogenesis inhibition while negating many of the undesirable consequences of inducing intratumoral hypoxia. As a result, combining FDA approved anti-angiogenic agents and PIM inhibitors has the potential to be translated to the clinical setting and impact patient outcomes.

Supplementary Material

Refer to Web version on PubMed Central for supplementary material.

Acknowledgements

We would like to thank Dr. Brenda Baggett for assisting with the acquisition and analysis of *in vivo* imaging experiments. We appreciate the support of Genentech for providing B20–4.1.1 for *in vivo* studies.

Financial Support: This research was supported by ACS grant RSG-16–159-01-CDD to N.A.W. and NIH R01 CA173200 and DOD W81XWH-12–1-0560 to A.S.K. Cancer center support grant P30CA023074 also provided support for this research.

References

1. Hanahan D, Weinberg RA. Hallmarks of cancer: the next generation. Cell. 2011;144:646–74. [PubMed: 21376230]
2. Semenza GL. Regulation of cancer cell metabolism by hypoxia-inducible factor 1.Semin Cancer Biol. 2009;19:12–6. [PubMed: 19114105]
3. Dvorak HF, Brown LF, Detmar M, Dvorak AM. Vascular permeability factor/vascular endothelial growth factor, microvascular hyperpermeability, and angiogenesis. The American journal of pathology. 1995;146:1029–39. [PubMed: 7538264]
4. Rosen LS. Clinical experience with angiogenesis signaling inhibitors: focus on vascular endothelial growth factor (VEGF) blockers. Cancer Control. 2002;9:36–44. [PubMed: 11965229]
5. Hurwitz H, Fehrenbacher L, Novotny W, Cartwright T, Hainsworth J, Heim W, et al. Bevacizumab plus irinotecan, fluorouracil, and leucovorin for metastatic colorectal cancer. N Engl J Med. 2004;350:2335–42. [PubMed: 15175435]
6. Johnson DH, Fehrenbacher L, Novotny WF, Herbst RS, Nemunaitis JJ, Jablons DM, et al. Randomized phase II trial comparing bevacizumab plus carboplatin and paclitaxel with carboplatin and paclitaxel alone in previously untreated locally advanced or metastatic non-small-cell lung cancer. Journal of clinical oncology : official journal of the American Society of Clinical Oncology. 2004;22:2184–91. [PubMed: 15169807]

7. Yang JC. Bevacizumab for patients with metastatic renal cancer: an update. Clinical cancer research : an official journal of the American Association for Cancer Research. 2004;10:6367S–70S. [PubMed: 15448032]
8. Franco M, Man S, Chen L, Emmenegger U, Shaked Y, Cheung AM, et al. Targeted anti-vascular endothelial growth factor receptor-2 therapy leads to short-term and long-term impairment of vascular function and increase in tumor hypoxia. Cancer Res. 2006;66:3639–48. [PubMed: 16585189]
9. Mehta S, Hughes NP, Buffa FM, Li SP, Adams RF, Adwani A, et al. Assessing early therapeutic response to bevacizumab in primary breast cancer using magnetic resonance imaging and gene expression profiles. J Natl Cancer Inst Monogr. 2011;2011:71–4. [PubMed: 22043045]
10. Willett CG, Boucher Y, di Tomaso E, Duda DG, Munn LL, Tong RT, et al. Direct evidence that the VEGF-specific antibody bevacizumab has antivascular effects in human rectal cancer. Nat Med. 2004;10:145–7. [PubMed: 14745444]
11. McIntyre A, Harris AL. Metabolic and hypoxic adaptation to anti-angiogenic therapy: a target for induced essentiality. EMBO Mol Med. 2015;7:368–79. [PubMed: 25700172]
12. DeLay M, Jahangiri A, Carbonell WS, Hu YL, Tsao S, Tom MW, et al. Microarray analysis verifies two distinct phenotypes of glioblastomas resistant to antiangiogenic therapy. Clin Cancer Res. 2012;18:2930–42. [PubMed: 22472177]
13. Bergers G, Hanahan D. Modes of resistance to anti-angiogenic therapy. Nat Rev Cancer. 2008;8:592–603. [PubMed: 18650835]
14. Semenza GL. Hydroxylation of HIF-1: oxygen sensing at the molecular level. Physiology (Bethesda). 2004;19:176–82. [PubMed: 15304631]
15. Bruick RK, McKnight SL. A conserved family of prolyl-4-hydroxylases that modify HIF. Science. 2001;294:1337–40. [PubMed: 11598268]
16. Ivan M, Kondo K, Yang H, Kim W, Valiando J, Ohh M, et al. HIFalpha targeted for VHL-mediated destruction by proline hydroxylation: implications for 02 sensing. Science. 2001;292:464–8. [PubMed: 11292862]
17. Maxwell PH, Wiesener MS, Chang GW, Clifford SC, Vaux EC, Cockman ME, et al. The tumour suppressor protein VHL targets hypoxia-inducible factors for oxygen-dependent proteolysis. Nature. 1999;399:271–5. [PubMed: 10353251]
18. Wenger RH, Stiehl DP, Camenisch G. Integration of oxygen signaling at the consensus HRE. Sci STKE. 2005;2005:re12.
19. Rankin EB, Giaccia AJ. The role of hypoxia-inducible factors in tumorigenesis. Cell Death Differ. 2008;15:678–85. [PubMed: 18259193]
20. Hartwich J, Orr WS, Ng CY, Spence Y, Morton C, Davidoff AM. HIF-1 alpha activation mediates resistance to anti-angiogenic therapy in neuroblastoma xenografts. J Pediatr Surg. 2013;48:39–46. [PubMed: 23331791]
21. Liu HT, Wang N, Wang X, Li SL. Overexpression of Pim-1 is associated with poor prognosis in patients with esophageal squamous cell carcinoma. J Surg Oncol. 2010;102:683–8. [PubMed: 20544717]
22. Dhanasekaran SM, Barrette TR, Ghosh D, Shah R, Varambally S, Kurachi K, et al. Delineation of prognostic biomarkers in prostate cancer. Nature. 2001;412:822–6. [PubMed: 11518967]
23. Xie Y, Xu K, Dai B, Guo Z, Jiang T, Chen H, et al. The 44 kDa Pim-1 kinase directly interacts with tyrosine kinase Etk/BMX and protects human prostate cancer cells from apoptosis induced by chemotherapeutic drugs. Oncogene. 2006;25:70–8. [PubMed: 16186805]
24. Nawijn MC, Alendar A, Berns A. For better or for worse: the role of Pim oncogenes in tumorigenesis. Nat Rev Cancer. 2011;11:23–34. [PubMed: 21150935]
25. Lu J, Zavorotinskaya T, Dai Y, Niu XH, Castillo J, Sim J, et al. Pim2 is required for maintaining multiple myeloma cell growth through modulating TSC2 phosphorylation. Blood. 2013;122:1610–20. [PubMed: 23818547]
26. Keeton EK, McEachern K, Dillman KS, Palakurthi S, Cao Y, Grondine MR, et al. AZD1208, a potent and selective pan-Pim kinase inhibitor, demonstrates efficacy in preclinical models of acute myeloid leukemia. Blood. 2014;123:905–13. [PubMed: 24363397]

27. Warfel NA, Sainz AG, Song JH, Kraft AS. PIM Kinase Inhibitors Kill Hypoxic Tumor Cells by Reducing Nrf2 Signaling and Increasing Reactive Oxygen Species. Mol Cancer Ther. 2016.
28. Kondo K, Klco J, Nakamura E, Lechpammer M, Kaelin WG, Jr. Inhibition of HIF is necessary for tumor suppression by the von Hippel-Lindau protein. Cancer Cell. 2002;1:237–46. [PubMed: 12086860]
29. Emerling BM, Weinberg F, Liu JL, Mak TW, Chandel NS. PTEN regulates p300- dependent hypoxia-inducible factor 1 transcriptional activity through Forkhead transcription factor 3a (F0X03a). Proc Natl Acad Sci USA. 2008;105:2622–7. [PubMed: 18268343]
30. Safran M, Kim WY, O'Connell F, Flippin L, Gunzler V, Horner JW, et al. Mouse model for noninvasive imaging of HIF prolyl hydroxylase activity: assessment of an oral agent that stimulates erythropoietin production. Proc Natl Acad Sci USA. 2006;103:105–10. [PubMed: 16373502]
31. Albers J, Danzer C, Rechsteiner M, Lehmann H, Brandt LP, Hejhal T, et al. A versatile modular vector system for rapid combinatorial mammalian genetics. J Clin Invest. 2015;125:1603–19. [PubMed: 25751063]
32. Mikkers H, Nawijn M, Allen J, Brouwers C, Verhoeven E, Jonkers J, et al. Mice deficient for all PIM kinases display reduced body size and impaired responses to hematopoietic growth factors. Mol Cell Biol. 2004;24:6104–15. [PubMed: 15199164]
33. Song JH, An N, Chatterjee S, Kistner-Griffin E, Mahajan S, Mehrotra S, et al. Deletion of Pim kinases elevates the cellular levels of reactive oxygen species and sensitizes to K-Ras- induced cell killing. Oncogene. 2014.
34. Iliopoulos O, Kibel A, Gray S, Kaelin WG, Jr. Tumour suppression by the human von Hippel-Lindau gene product. Nat Med. 1995;1:822–6. [PubMed: 7585187]
35. Warfel NA, Niederst M, Stevens MW, Brennan PM, Frame MC, Newton AC. Mislocalization of the E3 ligase, beta-transducin repeat-containing protein 1 (beta-TrCP1), in glioblastoma uncouples negative feedback between the pleckstrin homology domain leucine- rich repeat protein phosphatase 1 (PHLPP1) and Akt. J Biol Chem. 2011;286:19777–88. [PubMed: 21454620]
36. Cespedes MV, Espina C, Garcia-Cabezas MA, Trias M, Boluda A, Gomez del Pulgar MT, et al. Orthotopic microinjection of human colon cancer cells in nude mice induces tumor foci in all clinically relevant metastatic sites. Am J Pathol. 2007;170:1077–85. [PubMed: 17322390]
37. Wang Z, Bhattacharya N, Mixter PF, Wei W, Sedivy J, Magnuson NS. Phosphorylation of the cell cycle inhibitor p21Cip1/WAF1 by Pim-1 kinase. Biochim Biophys Acta. 2002;1593:45–55. [PubMed: 12431783]
38. Jiang R, Wang X, Jin Z, Li K. Association of Nuclear PIM1 Expression with Lymph Node Metastasis and Poor Prognosis in Patients with Lung Adenocarcinoma and Squamous Cell Carcinoma. J Cancer. 2016;7:324–34. [PubMed: 26918046]
39. Chen WW, Chan DC, Donald C, Lilly MB, Kraft AS. Pim family kinases enhance tumor growth of prostate cancer cells. Mol Cancer Res. 2005;3:443–51. [PubMed: 16123140]
40. Krock BL, Skuli N, Simon MC. Hypoxia-induced angiogenesis: good and evil. Genes Cancer. 2011;2:1117–33. [PubMed: 22866203]
41. Semenza GL. Hydroxylation of HIF-1: oxygen sensing at the molecular level. Physiology (Bethesda). 2004;19:176–82. [PubMed: 15304631]
42. Ohh M, Park CW, Ivan M, Hoffman MA, Kim TY, Huang LE, et al. Ubiquitination of hypoxia-inducible factor requires direct binding to the beta-domain of the von Hippel-Lindau protein. Nat Cell Biol. 2000;2:423–7. [PubMed: 10878807]
43. Keunen O, Johansson M, Oudin A, Sanzey M, Rahim SA, Fack F, et al. Anti-VEGF treatment reduces blood supply and increases tumor cell invasion in glioblastoma. Proc Natl Acad Sci USA. 2011;108:3749–54. [PubMed: 21321221]
44. Yang Y, Zhang Y, Iwamoto H, Hosaka K, Seki T, Andersson P, et al. Discontinuation of anti-VEGF cancer therapy promotes metastasis through a liver revascularization mechanism. Nat Commun. 2016;7:12680. [PubMed: 27580750]
45. Hanahan D, Folkman J. Patterns and emerging mechanisms of the angiogenic switch during tumorigenesis. Cell. 1996;86:353–64. [PubMed: 8756718]

46. Ueda S, Saeki T, Osaki A, Yamane T, Kuji I. Bevacizumab induces acute hypoxia and cancer progression in patients with refractory breast cancer: Multimodal functional imaging and multiplex cytokine analysis. Clin Cancer Res. 2017.

47. Van der Veldt AA, Lubberink M, Bahce I, Walraven M, de Boer MP, Greuter HN, et al. Rapid decrease in delivery of chemotherapy to tumors after anti-VEGF therapy: implications for scheduling of anti-angiogenic drugs. Cancer Cell. 2012;21:82–91. [PubMed: 22264790]

48. Sennino B, Ishiguro-Oonuma T, Wei Y, Naylor RM, Williamson CW, Bhagwandin V, et al. Suppression of tumor invasion and metastasis by concurrent inhibition of c-Met and VEGF signaling in pancreatic neuroendocrine tumors. Cancer Discov. 2012;2:270–87. [PubMed: 22585997]

49. Cen B, Xiong Y, Song JH, Mahajan S, DuPont R, McEachern K, et al. The Pim-1 protein kinase is an important regulator of MET receptor tyrosine kinase levels and signaling. Mol Cell Biol. 2014;34:2517–32. [PubMed: 24777602]

50. Finley LW, Carracedo A, Lee J, Souza A, Egia A, Zhang J, et al. SIRT3 opposes reprogramming of cancer cell metabolism through HIF1 alpha destabilization. Cancer Cell. 2011;19:416–28. [PubMed: 21397863]

51. Hagen T, Taylor CT, Lam F, Moncada S. Redistribution of intracellular oxygen in hypoxia by nitric oxide: effect on HIF1 alpha. Science. 2003;302:1975–8. [PubMed: 14671307]

52. Sogawa K, Numayama-Tsuruta K, Ema M, Abe M, Abe H, Fujii-Kuriyama Y. Inhibition of hypoxia-inducible factor 1 activity by nitric oxide donors in hypoxia. Proc Natl Acad Sci USA. 1998;95:7368–73. [PubMed: 9636155]

Statement of Translational Relevance:

Anti-angiogenic agents that aim to disrupt tumor vasculature are currently approved for the treatment of solid tumors. However, patients rapidly develop resistance to these drugs, in large part due to hypoxia-mediated therapeutic resistance. This study demonstrates PIM kinase expression as a novel mechanism of resistance to anti-angiogenic agents. We show that PIM is upregulated following treatment with anti-VEGF therapies, and PIM expression reduces the ability of these drugs to effectively disrupt tumor vasculature. Combinatorial inhibition of PIM and VEGF produces a synergistic anti-tumor response that is characterized by enhanced cell death, growth arrest, decreased angiogenesis, and reduced metastasis. Small molecule PIM inhibitors reduce HIF-1 activity, opposing a shift to the pro-angiogenic gene signature associated with hypoxia. The unique ability of PIM inhibitors to concomitantly target angiogenesis and selectively kill hypoxic tumor cells addresses two major components of tumor progression and therapeutic resistance.

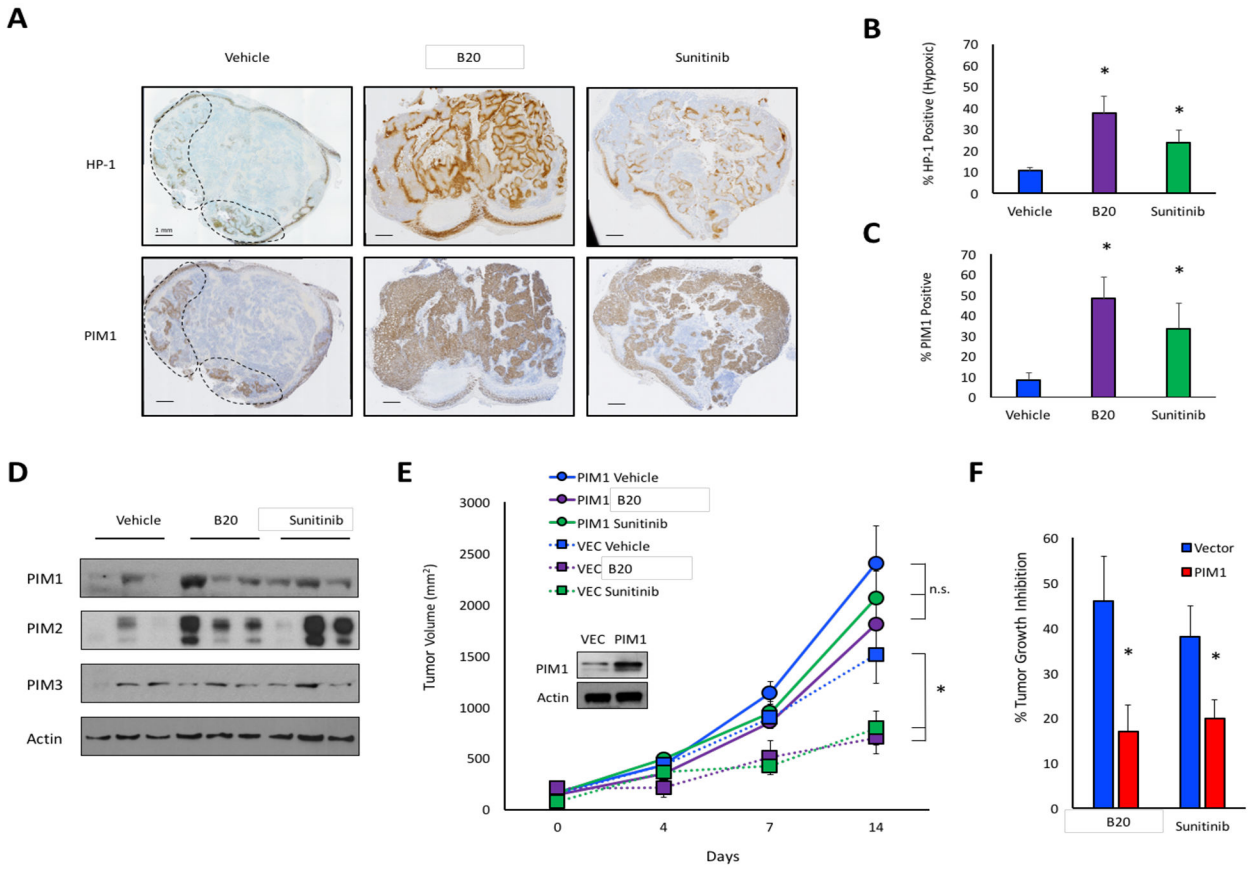

Figure 1. PIM1 expression is increased following treatment with anti-angiogenic agents *in vivo*.

A) Mice harboring PC3 prostate cancer xenograft tumors were treated with vehicle, B20–4.1.1, or sunitinib. Serial sections from tumors were immunostained to measure hypoxia (hypoxyprobe; HP-1) and PIM1 (dashed lines delineate regions of hypoxia). B) Percent HP-1 and C) percent PIM1 positivity was determined by microscopy. D) PIM isoform expression in each cohort was assessed by immunoblotting. E) Mice injected with PC3/VEC or PC3/PIM1 cells were treated with vehicle, B20–4.1.1, or sunitinib, and tumor volume was measured over time. F) Percent tumor growth inhibition in PC3/VEC and PC3/PIM1 following treatment with sunitinib or B20. *, $p < 0.05$; n.s. = not significant.

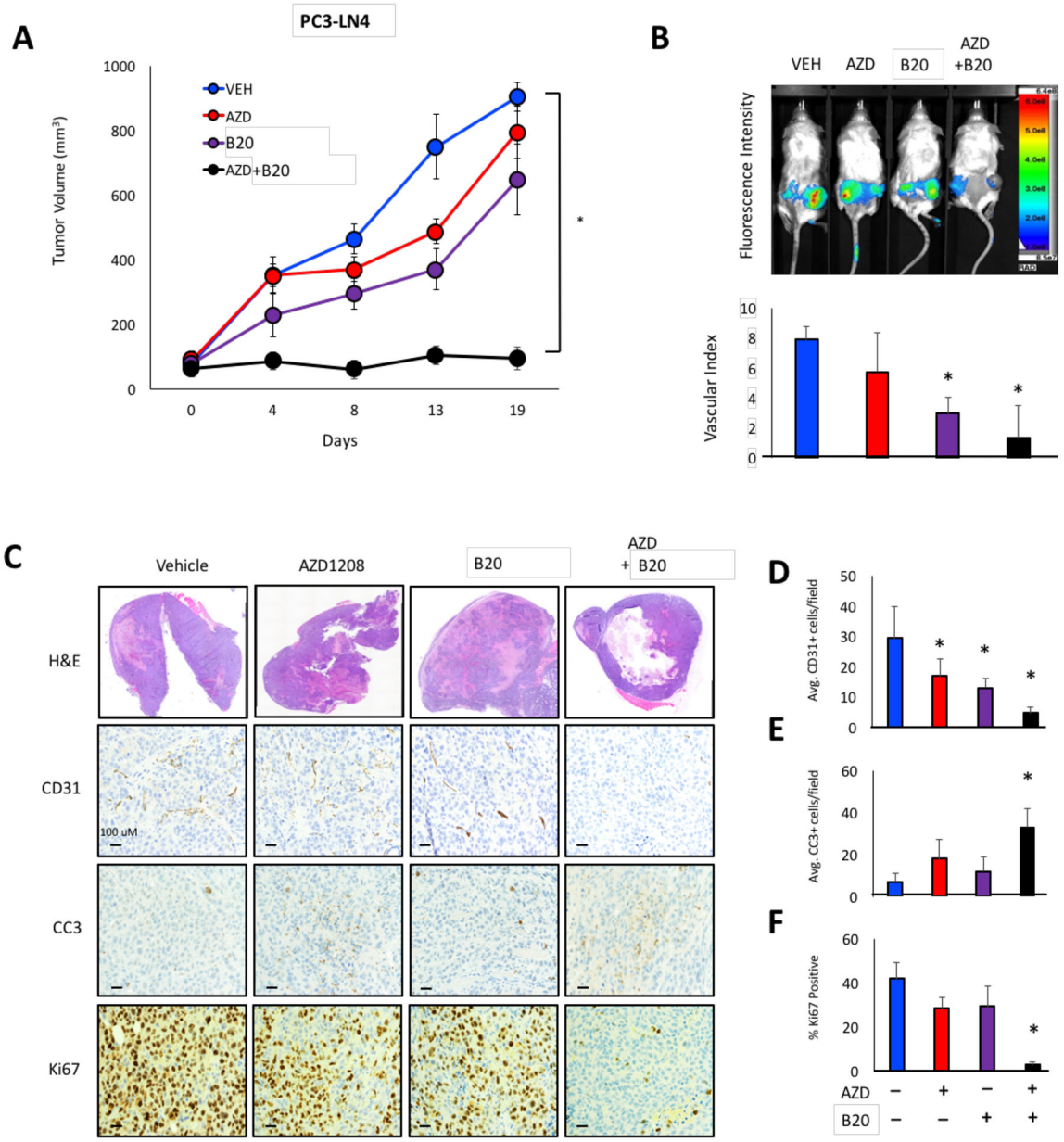

Figure 2. Combinatorial inhibition of PIM and VEGF produces synergistic anti-tumor activity.

A) Mice harboring PC3-LN4 tumors were treated with the indicated drugs, and tumor volume was measured over time. B) Mice were injected with Angiosense750EX (2 nmol) 24 h before imaging, and the vascular index was calculated by normalizing the bioluminescence signal to tumor volume. C) Tumors from each cohort were immunostained with CD31, cleaved caspase 3 (CC3), and Ki67 to measure angiogenesis, apoptosis, and proliferation, respectively. D-F) Quantification of CD31, CC3, and Ki67 staining in each cohort. *, $p < 0.05$ compared to vehicle.

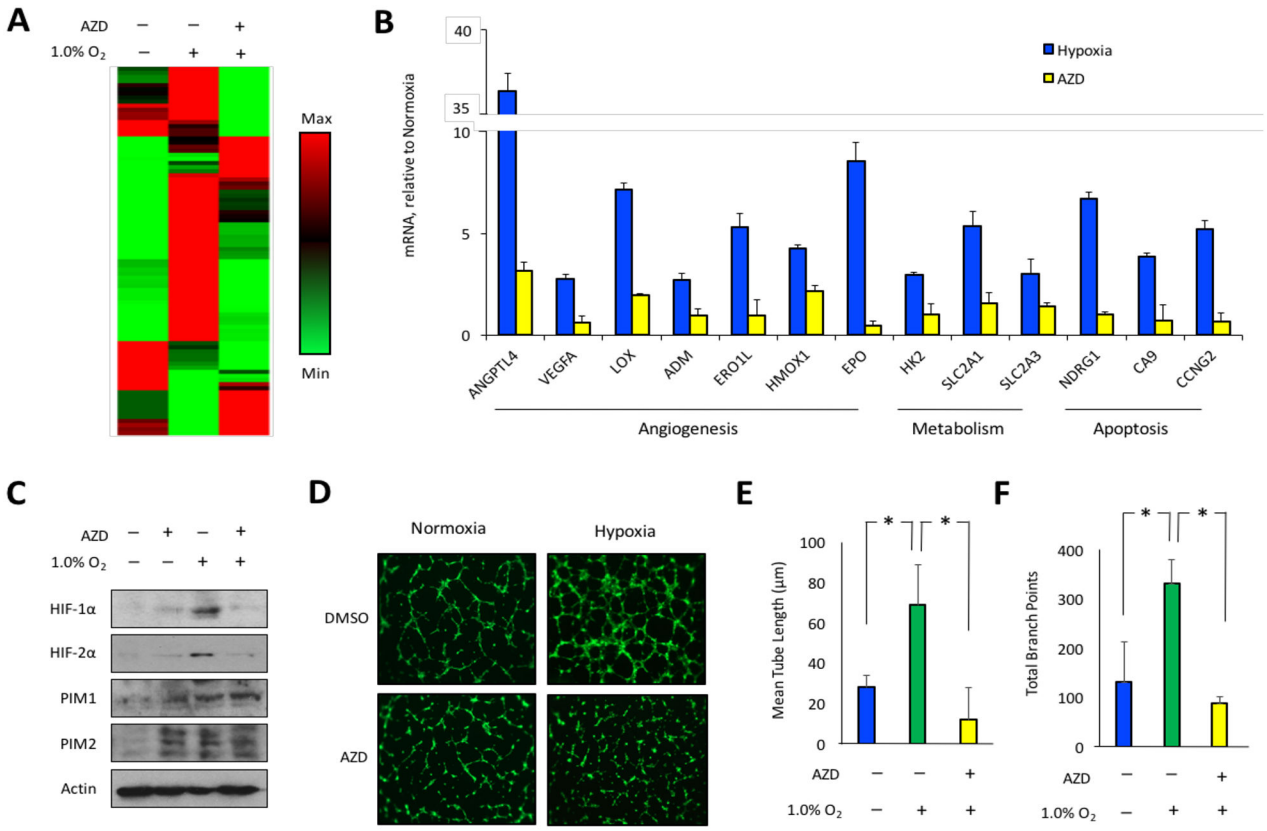

Figure 3. PIM inhibition opposes hypoxia-induced angiogenesis.

A) PC3 cells were incubated in normoxia or hypoxia ± AZD1208 (3 μM) for 8h and mRNA was collected to measure the expression of hypoxia-inducible genes. B) AZD1208 prevented the hypoxia-inducible expression of pro-angiogenic genes. C) PC3 cells were incubated in normoxia or hypoxia ± AZD1208 for 24 h, and lysates were collected to assess HIF1/2-α protein levels. D) Conditioned media were collected from the samples described in (C), and tube formation assays were performed as described in the methods section. E) Tube length and branching points were quantified at 6 h after plating. *, $p < 0.05$.

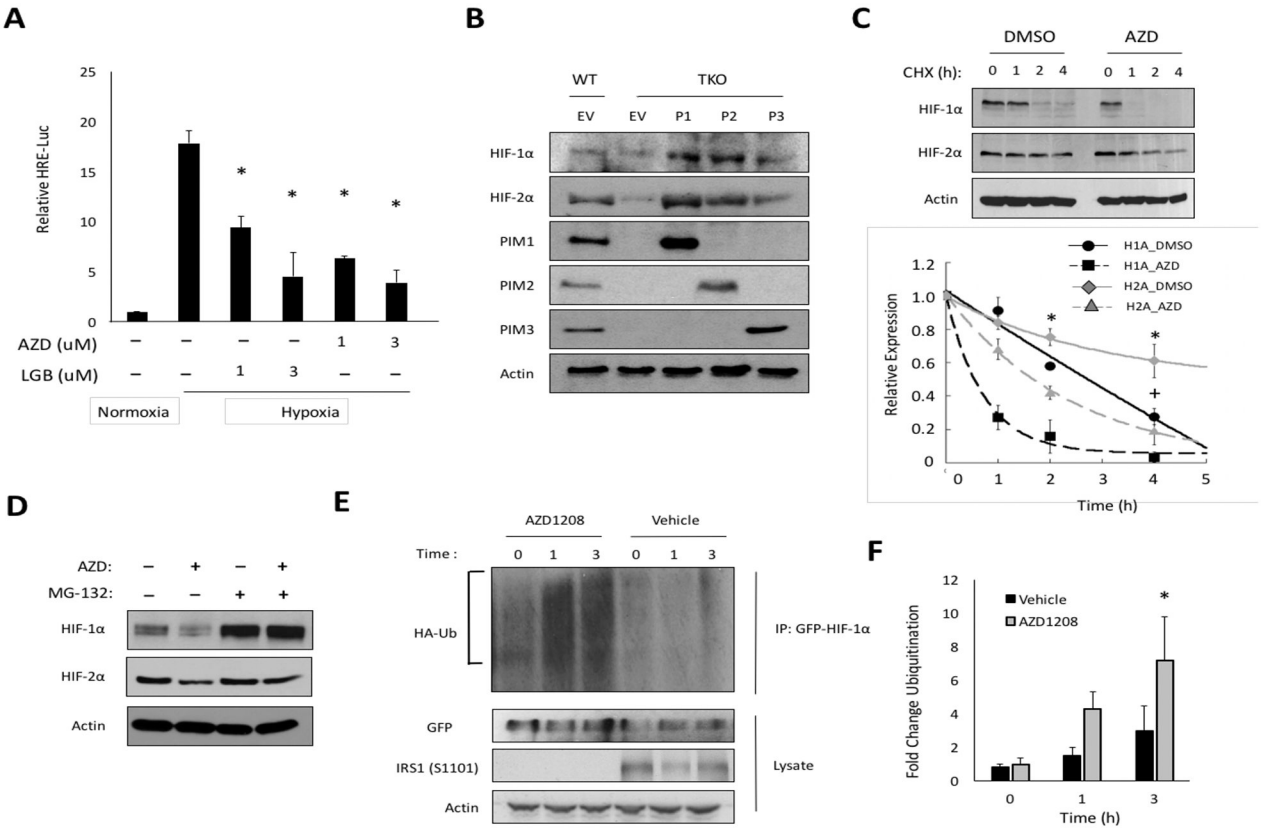

Figure 4. PIM inhibition reduces HIF-1/2α protein levels by enhancing their proteasomal degradation.

A) PC3-LN4 cells expressing HRE-Luc were incubated in normoxia or hypoxia ± AZD1208 or LGB321 for 6 h. B) The indicated cell lines were incubated for 6 h in hypoxia, and protein was collected to monitor HIF1/2-α levels. C) PC3-LN4 cells were cultured in hypoxia for 4 h prior to the addition of cycloheximide (CHX, 12.5 μg/mL). Lysates were harvested at the indicated time points, and densitometry was used to determine the rate of protein decay. D) PC3-LN4 cells were treated with MG-132 (5 μM), AZD1208 (3 μM), or a combination of both for 6 h in hypoxia. E) 293T cells were transfected with GPF-HIF-1α and HA-Ubiquitin and placed in hypoxia for 4 h prior to treatment with AZD1208. Cellular ubiquitination assays were performed, and F) densitometry was used to quantify relative ubiquitination. *, $p < 0.05$ compared to control.

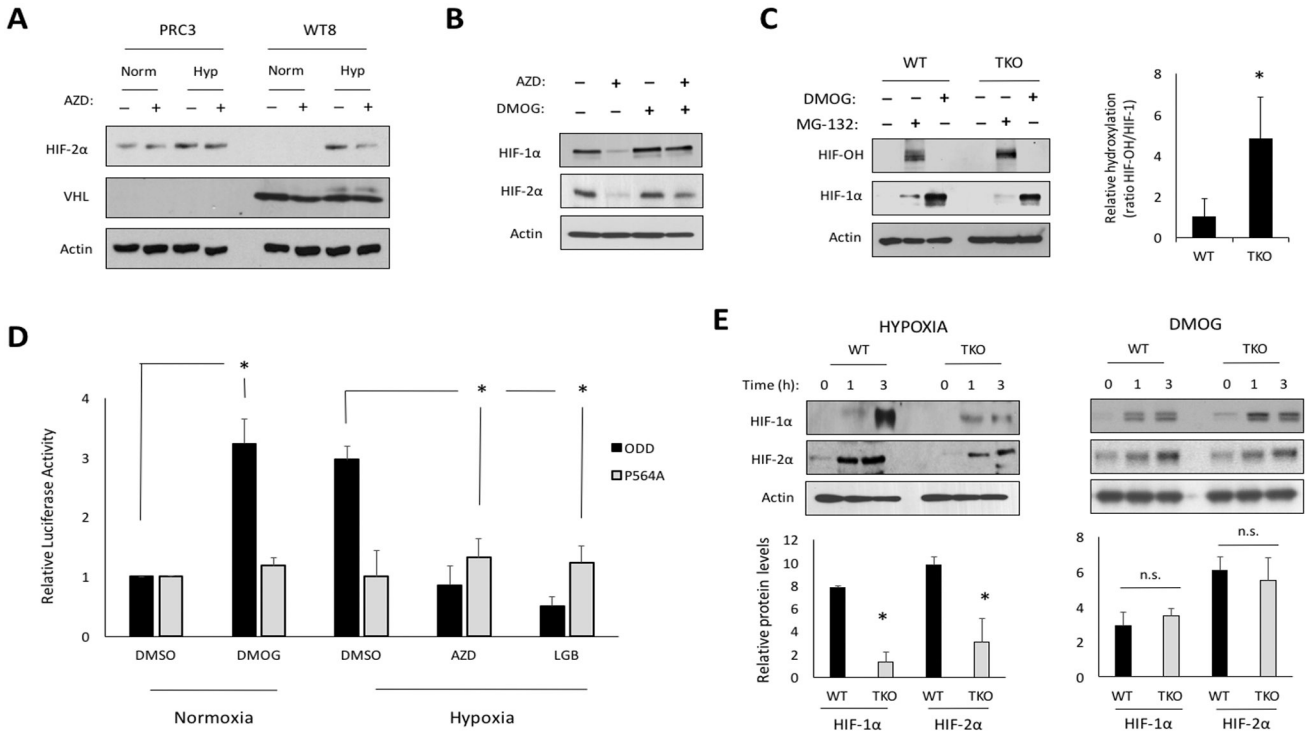

Figure 5. PIM inhibition increases PHD-mediated hydroxylation of HIF-1/2α isoforms.

A) 786-O cells expressing vector (PRC3) or VHL (WT8) were treated with vehicle or AZD1208 (3 μM) for 6 h in hypoxia. B) PC3-LN4 cells were treated with AZD, DMOG (1 mM), or both for 6 h in hypoxia. C) Lysates from wild type (WT) and PIM1/2/3 knockout (TKO) MEFs treated with or without MG-132 (10 μM) for 1 h or DMOG for 4 h were immunoblotted with antibodies specific to hydroxylated HIF-1α (HIF-OH) and total HIF-1α. D) PC3-LN4 cells transfected with the indicated ODD-Luc constructs were placed in normoxia or hypoxia for 6 h ± AZD1208 or LGB321 (1 μM). E) Western blots of WT and TKO MEF extracts cultured in hypoxia (1.0% O_2) or 1 mM DMOG for the indicated times. Densitometry was used to compare protein levels relative to time zero (bar graph). *, $p < 0.05$ compared to control; n.s. = not significant.

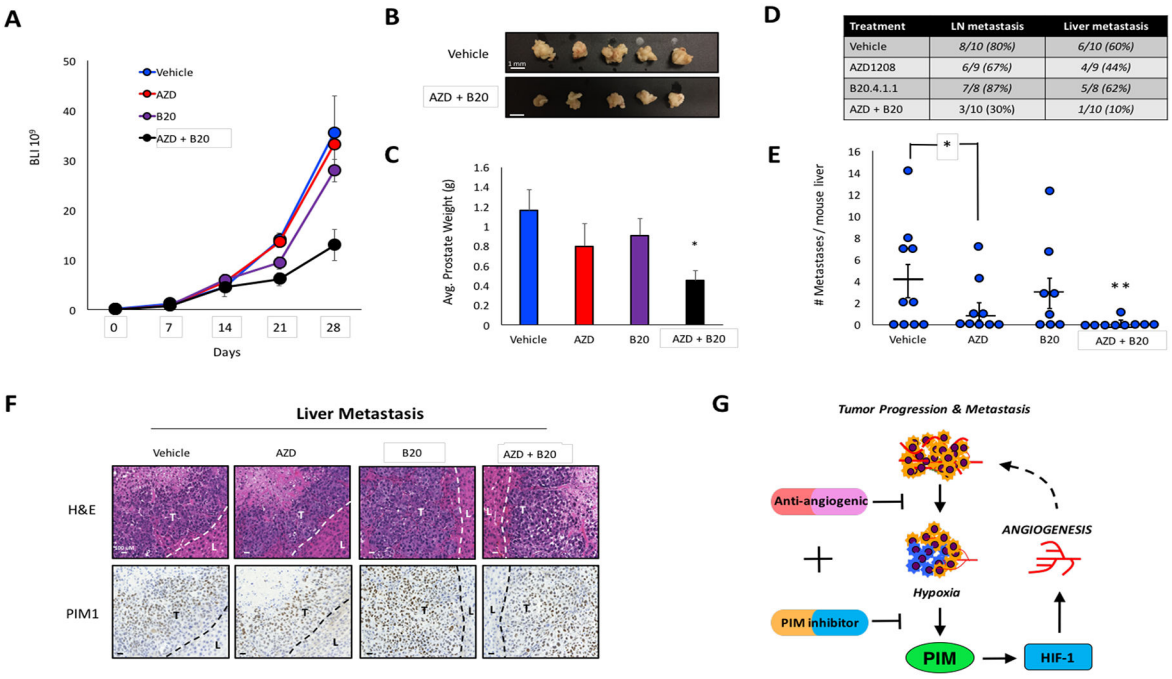

Figure 6. Simultaneous inhibition of PIM and VEGF reduces prostate cancer metastasis.

A) Orthotopic prostate tumors were treated as indicated, and the volume of the primary tumor was measured by bioluminescence over time. B) Images depicting the size difference between prostates from vehicle and AZD+B20 treated mice. C) Weight of prostates from each cohort after harvest. D) Incidence of lymph node and liver metastasis in each cohort. E) Livers from mice in each cohort were dissected and macroscopic metastases were counted. F) Immunohistochemical staining of PIM1 expression in liver metastases (dashed lines delineate separation between liver (L) and tumor (T) tissues). G) Model depicting the function of PIM in response to anti-angiogenic agents. VEGF inhibition increases tumor hypoxia. Consequently, PIM is upregulated and promotes resistance through the activation of HIF-1 and angiogenesis. *, $p < 0.05$ compared to control; **, $p < 0.05$ compared to all other groups.